

See discussions, stats, and author profiles for this publication at: <https://www.researchgate.net/publication/234883685>

Pulsed dc- and sine-wave-excited cold atmospheric plasma plumes: A comparative analysis

Article in *Physics of Plasmas* · April 2010

DOI: 10.1063/1.3381132

CITATIONS

71

READS

203

7 authors, including:



Xinpei Lu

Huazhong University of Science and Technology

170 PUBLICATIONS 6,465 CITATIONS

SEE PROFILE



Kostya Ostrikov

Queensland University of Technology

660 PUBLICATIONS 14,589 CITATIONS

SEE PROFILE



Y. Xian

Huazhong University of Science and Technology

59 PUBLICATIONS 1,175 CITATIONS

SEE PROFILE



Chengwei Zou

Shandong University

28 PUBLICATIONS 963 CITATIONS

SEE PROFILE

Some of the authors of this publication are also working on these related projects:



SJTU research [View project](#)



plasma medicine [View project](#)

Pulsed dc- and sine-wave-excited cold atmospheric plasma plumes: A comparative analysis

Q. Xiong,¹ X. P. Lu,^{1,a)} K. Ostrikov,^{2,b)} Y. Xian,¹ C. Zou,¹ Z. Xiong,¹ and Y. Pan¹

¹College of Electrical and Electronic Engineering, HuaZhong University of Science and Technology, WuHan, Hubei 430074, People's Republic of China

²Plasma Nanoscience Centre Australia (PNCA), CSIRO Materials Science and Engineering, P.O. Box 218, Lindfield, New South Wales 2070, Australia

(Received 26 January 2010; accepted 12 March 2010; published online 14 April 2010)

Cold atmospheric-pressure plasma plumes are generated in the ambient air by a single-electrode plasma jet device powered by pulsed dc and ac sine-wave excitation sources. Comprehensive comparisons of the plasma characteristics, including electrical properties, optical emission spectra, gas temperatures, plasma dynamics, and bacterial inactivation ability of the two plasmas are carried out. It is shown that the dc pulse excited plasma features a much larger discharge current and stronger optical emission than the sine-wave excited plasma. The gas temperature in the former discharge remains very close to the room temperature across the entire plume length; the sine-wave driven discharge also shows a uniform temperature profile, which is 20–30 degrees higher than the room temperature. The dc pulse excited plasma also shows a better performance in the inactivation of gram-positive *staphylococcus aureus* bacteria. These results suggest that the pulsed dc electric field is more effective for the generation of nonequilibrium atmospheric pressure plasma plumes for advanced plasma health care applications. © 2010 American Institute of Physics.

[doi:10.1063/1.3381132]

I. INTRODUCTION

Atmospheric pressure nonequilibrium plasmas (APNPs) have recently been of an enormous interest owing to their attractive features that make them indispensable in a variety of advanced applications. One of the most prominent features of the APNPs is their enhanced plasma chemistry at low gas temperatures. Their technological applications include biomedicine,^{1–5} surface modification,⁶ materials synthesis and processing,^{7,8} chemical decontamination,^{9,10} water purification,^{11,12} as well as absorption and reflection of electromagnetic radiation.¹³ Recently, open-air plasma jet devices, which are capable of generating nonequilibrium plasma plumes at atmospheric pressure, have attracted a major attention.^{14–21} Compared with traditional APNPs sources, which normally generate plasmas in areas limited by electrodes and also require customized discharge chambers, the cold plasma jets are free from these requirements and thus have better flexibility and other indisputable advantages in practical applications.

Driven by the exciting prospects for a range of commercial applications, several cold plasma jet devices have been designed.^{22–31} These plasmas can be generated by using nanosecond dc voltage pulses with kilohertz repetition frequencies as well as with sine-wave excitations in the kilohertz-to-megahertz range. Some of these plasma jet devices powered by different excitation sources are capable of generating a plasma plume expanding into the surrounding air for a few centimeters and even longer. One of the most

salient features of such discharges is that the gas temperature of the plasma plume can be close to room temperature. This feature significantly improves the potential of the cold atmospheric-pressure plasma plumes for applications in health care and biomedicine where microorganisms, cell, living tissues, membranes, etc. are very sensitive to the process temperature. Such plasmas generated using different power supply schemes have demonstrated remarkable results in a variety of applications, such as bacterial inactivation,^{32–40} wound care and healing,^{1,41} skin disease and cancer therapies,^{42–45} as well as food decontamination.^{46,47} However, it still remains unclear how exactly the choice of any particular excitation source affects the plasma performance in targeted applications. The clue to solve this problem is in the comparison of the electrical, optical, and thermal properties of the discharges and identifying the most effective application-specific factors such as neutral or charged species, heat, UV radiation, etc. This is why a comprehensive and systematic comparative analysis of the properties and performance of the most commonly used excitation sources (pulsed dc and sine-wave ac) is on the agenda. This analysis should be focused on the detailed studies of the discharge characteristics and highlighting the unique features the plasmas which in turn underpin the viability of the specific targeted applications.

In this paper, a plasma jet device of a single high-voltage (HV) electrode configuration is used and driven by either sine-wave ac or pulsed dc power supply. The working gas is helium and the gas flow rate is the same (2 l/min) in both cases. Here we study and compare the following five aspects of the two discharges: electrical properties, optical emission spectra, gas temperature, plasma dynamics, as well as bacte-

^{a)}Electronic mail: luxinpei@hotmail.com.

^{b)}Also at School of Physics, The University of Sydney, Sydney, NSW 2006, Australia.

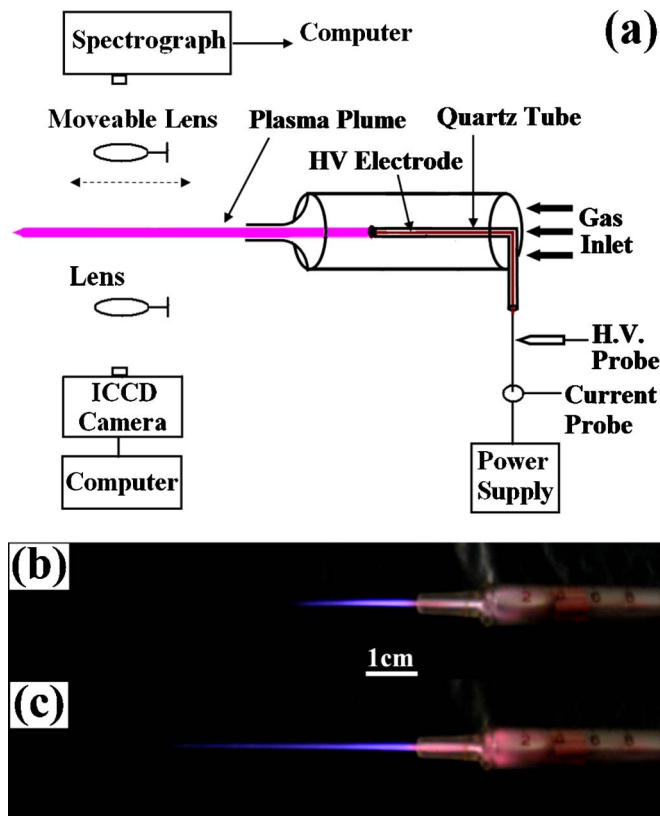


FIG. 1. (Color online) (a) Schematic of the experimental setup. Photographs of the helium plasma plumes powered by the (b) ac power supply with a peak-to-peak voltage of 16 kV and (c) pulsed dc power supply at 8 kV with pulse width of 800 ns. Both at a repetition rate of 4 kHz, and a helium gas flow rate of 2 l/min.

ricidal effectiveness. The rest of the paper is organized as follows. The experimental setup is described in Sec. II. Section III presents the experimental results related to the above five aspects. The discussion of the experimental results is given in Sec. IV. Finally, Sec. V presents a summary of this work and a brief outlook for the future research.

II. EXPERIMENTAL SETUP

Figure 1(a) is a schematic of the experimental setup. The plasma jet device studied in this paper has been reported previously.²² It is comprised of a medical-grade glass syringe, a quartz tube with one end closed, and a single HV electrode. The HV electrode made of a copper wire is inserted into the quartz tube; the electrode and the tube are aligned along the syringe axis. More detailed descriptions can be found in our previous reports.

When the helium gas is introduced into the syringe and a HV is applied to the HV electrode, a homogeneous plasma jet is generated inside the syringe and in the surrounding air. In order to study and compare the characteristics of the plasma sustained by the pulsed and sinusoidal excitation sources, two kinds of excitation sources were used. The first excitation source is based on a pulsed dc power supply with amplitudes up to 10 kV, repetition rate up to 10 kHz, and pulse width variable from 200 ns to dc. The other way of the plasma creation relied on a sine-wave ac power supply with

a peak-peak voltage up to 30 kV and a fixed frequency of 4 kHz. In this work, the operating parameters of the pulsed dc excitation sources were set at 8 kV for the applied voltage, 800 ns for the pulse width and 4 kHz for the frequency. Similarly, the peak-peak voltage and frequency of the sine-wave ac source were set at 16 kV and 4 kHz, respectively. For convenience, the plasmas produced by these two excitation sources will further be referred to as the pulsed dc plasmas (PDCPs) and sine-wave excited plasmas (SWEPs), respectively. Figures 1(b) and 1(c) show the photographs of the plasma plumes in the open air driven by the ac and pulsed dc excitation sources, respectively. As can be seen, the SWEPP plume [Fig. 1(b)] is clearly shorter than the pulsed dc-excited plasma plume [Fig. 1(c)].

The voltages and currents have been measured using a Tektronix P6015 voltage probe and a Tektronix TCP202 current probe, respectively. The signals collected by the probes have been recorded by a digital Tektronix DPO7104 oscilloscope. The optical emission spectra of these two plasma plumes have been measured by a half meter spectrometer (Princeton Instruments Acton SpectraHub 2500i). For the measurements in the spectral range from 200 to 800 nm, the grating and the slit width of the spectrometer have been set at 1200 groove/mm and 200 μm , respectively. Moreover, for the high-resolution spectroscopy of the nitrogen second positive system, the grating of 3600 g/mm and slit width of 80 μm have been used. An intensified charge coupled device (ICCD) camera (Princeton Instruments, model PIMAX2) has been used to capture the dynamics of the plasma plumes. For the high-speed imaging, the exposure time of the ICCD camera was set at 20 ns.

III. EXPERIMENTAL RESULTS

In this section, comparisons of the characteristics of the pulsed dc- and SWEPP plumes are presented. First, the current-voltage (I-V) characteristics of the two plasma discharges are compared, as well as their power consumptions. Then, in order to identify the various reactive species generated by these two plasma plumes, the optical emission spectra measurements have been carried out. Likewise, based on the best fit of the simulated spectra of the $C^3\Pi_u-B_3\Pi_g$ ($\Delta v = -2$) band transition of nitrogen and the experimentally recorded spectra, the rotational temperature (that characterizes the gas temperature of the plasma) and the vibrational temperature of the two plasma plumes are estimated. Meanwhile, high-speed imaging is also applied to study the dynamics of the two plasma plumes in the open air. Finally, the inactivation treatments of bacteria samples are carried out to study the application efficiency of the pulsed dc- and the sine-wave-excited plasma plumes in the biomedical applications.

A. Electrical characterization

Figure 2 shows the current-voltage characteristics of the pulsed dc-excited plasma plume at 8 kV and the sine-wave-excited plasma plume with a peak-to-peak voltage of 16 kV. It should be noticed that the current shown in Fig. 2(a) is the actual discharge current of the pulsed dc-excited helium dis-

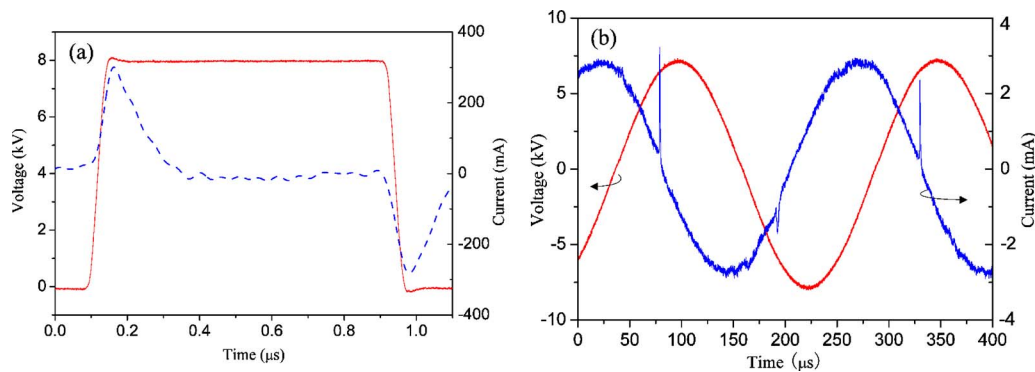


FIG. 2. (Color online) I-V characteristics of the helium discharges excited by the (a) pulsed dc power supply and (b) ac power supply. The discharge operation parameters are the same as in Fig. 1.

charge. This current was obtained by subtracting the displacement current (no helium flow, no plasma) from the total current (plasma is on). However, this subtraction method is not suitable for the sine-wave-excited case due to the instability of the discharge, which always induces phase shift of the measured current waveform. The current shown in Fig. 2(b) has a significant contribution of displacement current, and the sharp pulse represents the discharge current induced by the plasma. As can be seen from this figure, there are two distinct discharge current pulses characterizing the positive and negative breakdowns per cycle of the applied voltage for the both helium discharges. It is clearly seen that the peak value of the discharge current of the pulsed dc-excited plasma is much higher than that of the sine-wave-excited plasma.

It should be pointed out that the breakdown mechanism during the negative voltage cycles (for simplicity termed a “negative breakdown”) is quite different for the two cases. In the pulsed dc case, the negative breakdown is generated at the falling edge of the voltage pulse, and is induced by the charges accumulated on the dielectric electrode during the positive voltage phases of the discharge. The negative current pulse reaches its peak after the voltage pulse reduces to the minimum. This means that the negative breakdown is ignited without much energy input from the external circuit because the applied voltage is almost off during the negative voltage phase. The power consumed for igniting the positive discharge is partially stored for the negative breakdown during the negative voltage phase. This process ultimately improves the power efficiency for the plasma generation.

However, these distinctive discharge phases do not occur under the ac sine-wave excitation. The negative discharge of the SWEP is attributed to the polarity inversion of the external electric field. Therefore, the generation efficiency of the plasmas sustained by the pulsed dc electric field will be greater than in the sine-wave case. This is also supported by the following estimates of the power consumption in these two kinds of discharges. The average power deposited in the pulsed dc-excited plasma

$$P = 1/T \int_0^T u(t)i(t)dt,$$

is estimated to be about 1.8 W per voltage period, where T is the period of the applied voltage of 250 μ s. However, this

method is not suitable for the sine-wave excitation case because of the persistent shift of the measured current waveform, which is induced by the instability of the discharge. The displacement current does not show a 90° phase shift with respect to the applied voltage. Also, significant errors may arise in calculating the average power consumption by integrating the oscillograms of the applied voltage and the total current. Therefore, in order to estimate the power consumption of the SWEPs in a more accurate way, we applied the Lissajous-figure method by using a removable capacitor installed in front of the plasma plume. A relatively large grounded capacitor (1 nF) was installed close to the tip of the plasma plume as far as reasonably possible to obtain the minimum distortion of the discharge conditions. The distance of the capacitor away from the syringe nozzle is about 2.8 cm, slightly larger than the 2.4 cm of the length of the plasma plume. Then the measured voltage drop, $u_C(t)$, across the 1 nF capacitor, is used to calculate the charge, $Q(t)$, generated in the discharge inside the syringe and in the surrounding air (plasma plume) through the following equation:

$$u_C(t) = 1/C \int_{t_1}^{t_2} i(t)dt = Q(t)/C.$$

The average power consumed by the sine-wave-excited helium discharge can be determined from Lissajous figures. Figure 3 shows a typical Lissajous ellipsoid, which relates the charge $Q(t)$ to the applied voltage $u(t)$ during a single period of the applied voltage. The average power consumed by the SWEP during one voltage cycle is estimated to be about 3.5 W by calculating the area of the Lissajous figure, approximately two times higher than in the pulsed dc case.

B. Optical emission

Optical emission spectroscopy was applied to identify the excited species generated by the two plasma plumes in the wavelength range from 200 to 800 nm. Figures 4(a) and 4(b) and Figs. 4(c) and 4(d) show the optical emission spectra of the PDCPs and SWEPs, respectively. The optical emission was collected from the same position of the two plasma plumes about 5 mm away from the exit of the syringe nozzle. It is clearly seen that in addition to the atomic helium lines, the hydroxyl line (309 nm), the molecular nitrogen N_2 and molecular nitrogen ion N_2^+ rotational bands, and the atomic

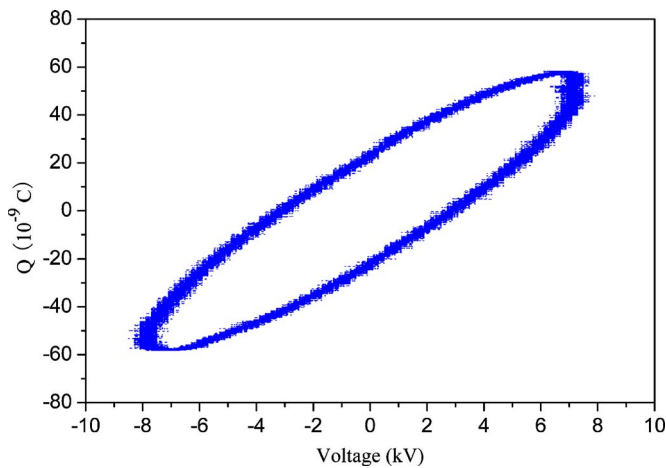


FIG. 3. (Color online) Lissajous figure for the helium discharge driven by the ac power supply. The discharge operation parameters are the same as in Fig. 1.

oxygen line (777.3 nm) appear in the spectra. In the wavelength range from 200 to 500 nm, the optical emission spectra are dominated by the N_2 and N_2^+ lines, whereas in the range from 500 to 800 nm by the atomic helium lines.

The nitrogen and oxygen lines are observed because of the air diffusion into the helium stream. Most of the emission lines of the pulsed dc-excited plasma plume are stronger than in the SWEP. It is remarkable that the emission intensity of the molecular nitrogen ion at 391.4 nm and the atomic oxygen at 777.3 nm, the intensity ratio in the PDCP and SWEP cases are also of the order of 2. The stronger emission intensity clearly indicates that more charges and reactive species are generated in the pulsed dc case. This further suggests that

higher-density and larger-volume open-air plasmas are generated in this case as compared with the SWEPs.

C. Rotational and vibrational temperatures of the plasma

The rotational temperature of nitrogen is normally accepted as an accurate estimate of the gas temperature of the atmospheric pressure plasmas. In this paper, the emission spectra of the second positive system of nitrogen are used to determine the rotational and vibrational temperatures of the two plasma plumes. By fitting the synthetic spectrum to the experimental spectrum of the $C^3\Pi_u-B_3\Pi_g$ ($\Delta v=-2$) band transition of nitrogen in the range from 368 to 383 nm, the rotational and vibrational temperatures of nitrogen can be obtained. Figure 5 shows the spatially resolved rotational and vibrational temperatures of the two plasma plumes in the open air. As can be seen, the both plasma plumes are characterized with a low rotational temperature [Fig. 5(a)] and a high vibrational temperature [Fig. 5(b)], and therefore are under strongly nonequilibrium conditions. The rotational temperature of the sine-wave-excited plasma plume is about 30 K higher than that of the PDCPs. This is also confirmed by using an infrared thermometer to measure the gas temperature of the two plasma plumes. It should be noted that the gas temperature of the sine-wave-excited plasma plume is unstable and can easily be increased by placing a treatment target closer to the nozzle.

Temperature estimates of these two plasma plumes connected to the ground through the same 1 M Ω resistor, which was fixed a distance of 20 mm in front of the syringe nozzle, have also been carried out. It is found that in this case the rotational temperature for the sine-wave-excited plasma

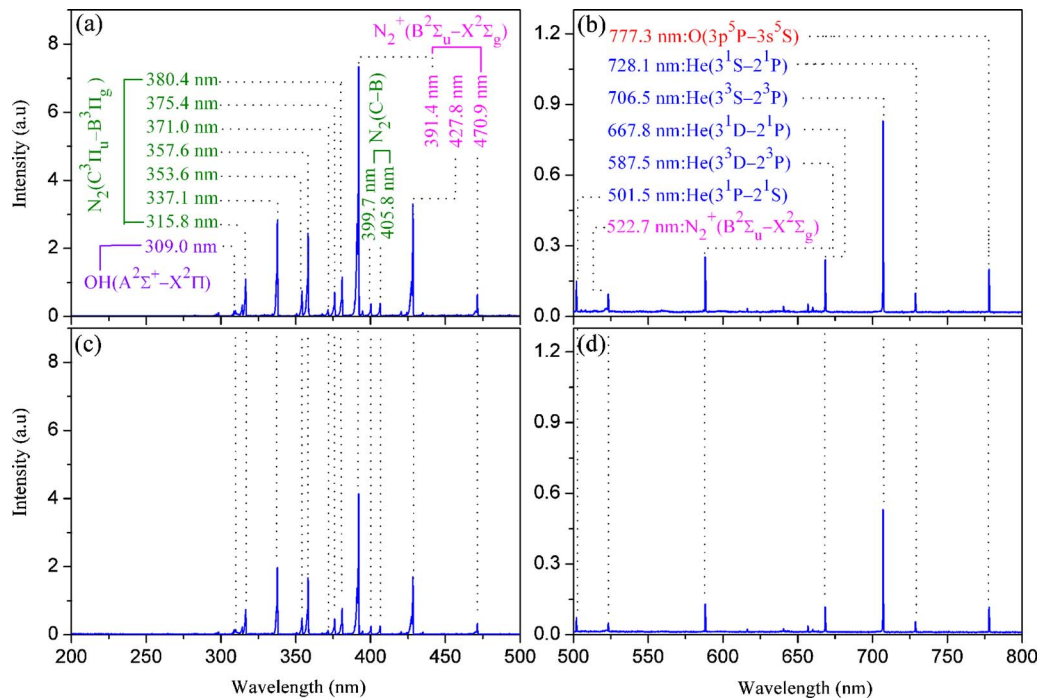


FIG. 4. (Color online) Optical emission spectrum in the range from 200 to 800 nm of the helium plasmas in the open air driven by the [(a) and (b)] pulsed dc power supply and [(c) and (d)] ac power supply. The discharge operation parameters are the same as in Fig. 1.

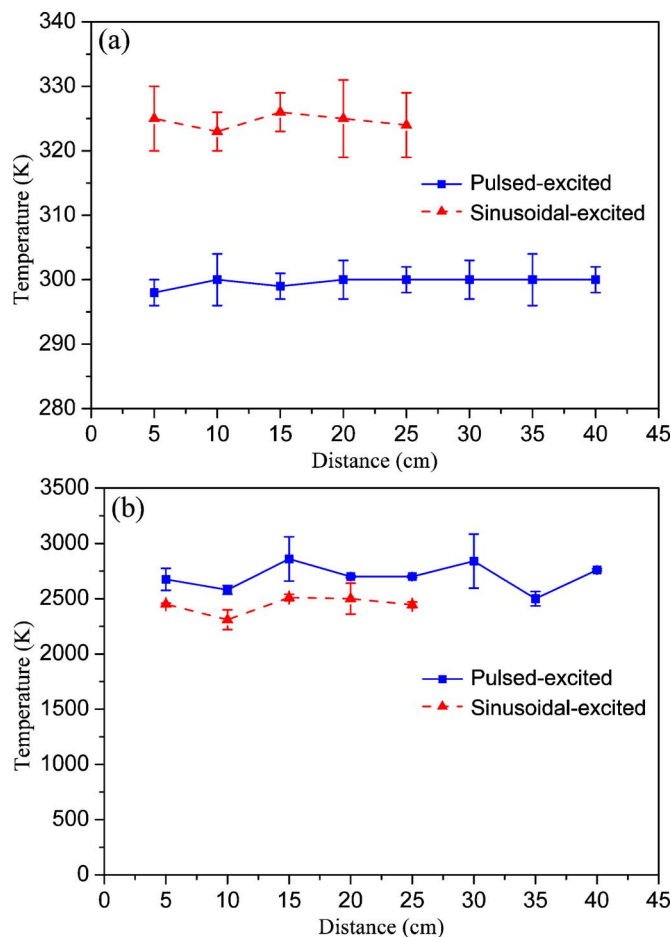


FIG. 5. (Color online) Spatially resolved (a) rotational and (b) vibrational temperatures of the helium plasma plumes in the open air driven by the pulsed dc and ac power supplies. The discharge operation parameters are the same as in Fig. 1.

plume increases up to about 400 K. On the contrary, the plume temperature remains close to room temperature for the pulsed dc-excited plasmas. Thus, the gas temperature of the PDCPs is much more stable than in the case of the sine-wave excitation. Furthermore, this is a clear indication that the pulsed dc-excited plasma plume is much better suited for temperature-sensitive biomedical applications compared with the sine-wave-excited plasmas.

D. Bullets behavior

High-speed imaging was applied to capture the dynamics of the plasma plumes in the open air. Figure 6 shows the behaviors of the plasma bullet behavior in the two cases of our interest in this work. The time delay marked in Figs. 6(a) and 6(b) corresponds to the onset of the applied voltage pulses and the positive phases of the sine-wave signals, respectively. As can be seen from this figure, the plasma bullets of the pulsed dc-excited plasma plume [Fig. 6(a)] have relatively large semi-spherical ionization fronts. On the other hand, the ac-excited plasma plume [Fig. 6(b)] has a shape of a long, narrow plasma channel. The spatial distribution of the bullet velocity of the two plasma plumes is shown in Fig. 7. It is obvious that the plasma bullets propagate more rapidly

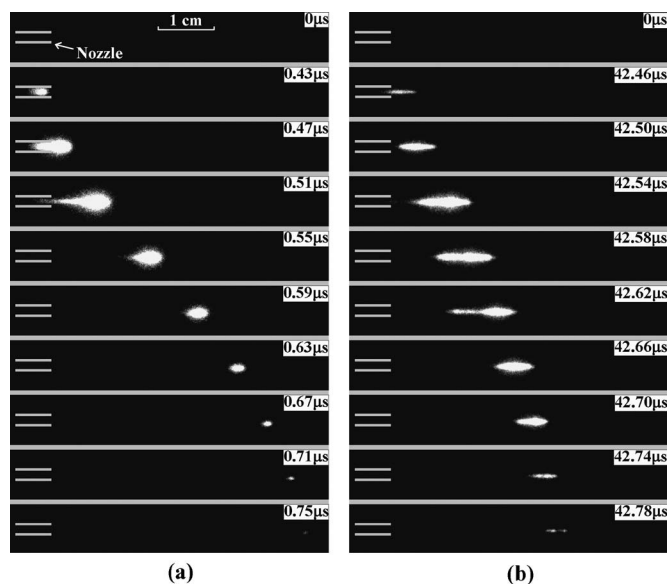


FIG. 6. The dynamics of the (a) pulsed dc excited plasma plume and (b) its sine-wave-excited counterpart. The discharge operation parameters are the same as in Fig. 1.

and to a longer distance in the open air in the pulsed dc excitation case. An interesting observation is that the ratio of the maximum bullet velocity in the two cases is also approximately 2.

E. Bacterial inactivation efficiency

To compare the efficiency of the pulsed dc- and sine-wave-excited plasma plumes in biomedical applications, the inactivation treatments of bacterial samples were carried out. A gram-positive *staphylococcus aureus* bacterium was chosen for this experiment. The bacterial samples treated by the two plasmas were prepared in the following sequence. First, a bacterial culture with the concentration about 10^8 cfu/ml (cfu: colony-forming unit) was prepared. Then this bacterial culture was placed into an oven for an overnight incubation at 37 °C. After that, the bacterial culture

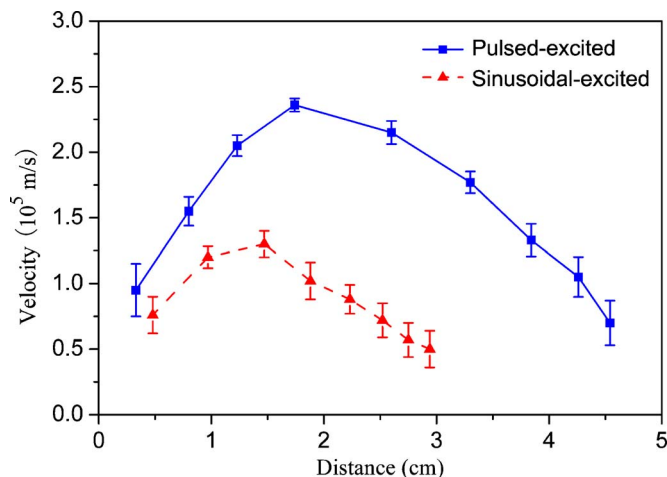


FIG. 7. (Color online) Spatial evolution of the bullet velocity of the pulsed dc- and sine-wave-excited plasma plumes. The discharge operation parameters are the same as in Fig. 1.

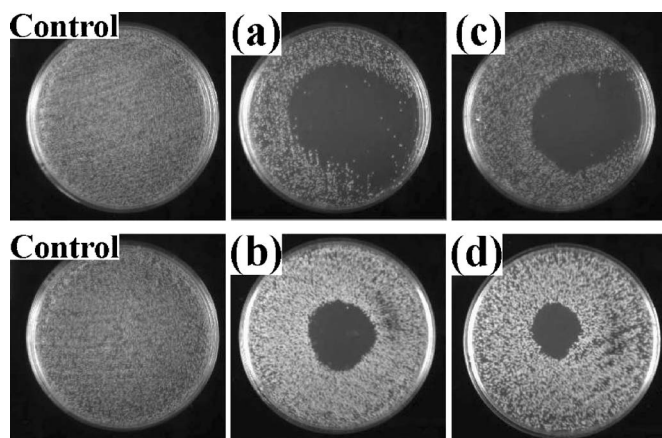


FIG. 8. Photographs of *staphylococcus aureus* bacterial samples on agar in Petri dishes after [(a) and (b)] direct and [(c) and (d)] indirect treatments by the helium plasma plumes driven by the [(a) and (c)] pulsed dc power supply and [(b) and (d)] ac power supply. The control experiment is also presented. The discharge operation parameters are the same as in Fig. 1.

was diluted to 10^6 cfu/ml. Finally, 200 μ l of the diluted suspension was extracted and then evenly spread over each agar plate in a Petri dish. We treated the bacterial samples through two different ways, namely, by direct and indirect plasma exposure. During the direct exposure process, the bacterial samples on the agar plates were placed right under the syringe nozzle; these samples were in a direct contact with the plasma plumes during the bacterial inactivation processes. In the indirect treatment process, a thin wire grounded through a 2 M Ω resistor was placed between the plasma nozzle and the bacterial samples. For more detailed descriptions about this two treatment ways can be found in our previous report.³³ After the plasma treatment, the bacterial samples on the agar plates in Petri dishes were put back into the oven and incubated for 24 h at 37 $^{\circ}$ C. For the control experiments, the bacterial samples were treated using a helium gas flow with the same gas flow rate as during the plasma discharges; in this case no HV was applied and the plasma was off.

Figure 8 shows the test results for the inactivation treatments of the bacterial samples by the two plasma plumes. The dark areas resembling uncontaminated agar suggest effective death of bacteria in these areas. On the other hand, the areas unaffected by the plasma treatment do not significantly change either their appearance or color, which is gray, similar to the control samples. It is quite possible that bacterial growth and reproduction continues in the latter areas. Figure 8 clearly shows the presence of the dark affected areas for the both cases of either direct or indirect treatments. Moreover, these areas are significantly larger in the PDCP case compared with the sine-wave-driven plasmas. This can be attributed to the more effective generation of reactive species in the PDCP plume, which in turn leads to the higher optical emission intensities [Figs. 4(a) and 4(b)]. These reactive species play a significant role in the inactivation process of bacterial samples. However, one should not conclude that the SWEPP is not suitable for bacterial inactivation applica-

tions. The treatment area of the SWEPPs is more localized, which can be crucial for a large number of applications where the locality of treatment is required.

IV. DISCUSSION

As shown in Fig. 2, the current of the helium discharge excited by the pulsed dc power source is much larger than in the sine-wave excitation case. It is known that the bullet velocity v_b can be quite high and can be characterized by the electron drift velocity v_d .^{48,49} One can observe in Fig. 6 that the bullet velocity v_b of the pulsed dc-excited plasma is higher compared with the ac excitation case. In this case, we obtain the estimate for the electron density n_e of the PDCPs. The electron density turns out to be at least two orders of magnitude higher than in the sine-wave-excited plasma case. This estimate follows from $n_e = J/ev_d$, where J is the current density. The large electron density is crucial for the generation of high-density reactive plasmas with high densities of reactive species created through electron impact processes. This is consistent with our observations that PDCPs produce a much stronger optical emission. Furthermore, this also suggests that the concentrations of reactive species in the pulsed dc-excited plasma plumes are significantly higher than in the sine-wave-excited plasmas.

Another obvious advantage of the pulsed dc discharge is that in PDCPs the electrons gain energy at much higher rates than in SWEPPs, mostly because of the very rapid (about 50 ns) rise-phase of the voltage pulses. The product of the gas pressure p and mobility of electron μ_e in pure helium is 0.86×10^6 cm² Torr/V s.⁵⁰ In our case, the applied voltage is 8 kV, and the pressure is 760 Torr, and the gap between the closed end of the quartz tube and gas inlet of the syringe nozzle is about 0.5 cm. Hence, the electron drift velocity can be estimated to be approximately 1.7×10^7 cm/s. In the case considered, the dominant ions are He⁺ and He₂⁺ in the plasma inside the syringe because of the low concentration of air impurity. The mobilities of He⁺ and He₂⁺ ions in pure helium at atmospheric pressure are 8 and 20 cm²/V s, respectively.⁵⁰ Under the same conditions, the drift velocities of He⁺ and He₂⁺ are about 1.3 and 3.2×10^5 cm/s, which is more than two orders of magnitude smaller than the electron drift velocity. Therefore, during this short rise-phase (about 50 ns), heavy ions have no time to respond to the electric field and remain almost static, and only electrons can follow the electric field. The electric field strength increases sharply as the applied voltage reaches its peak value. In this case the energy is transferred almost exclusively to the electrons, which in turn fairly coherently move along the direction of the external electric field. This is why a relatively high electron temperature can be achieved at a low gas (heavy particle) temperature. More importantly, under such conditions the plasma is extremely nonequilibrium. This nonequilibrium in turn leads to markedly higher rates of the ionization, excitation, and dissociation processes thus eventually resulting in the significantly enhanced plasma reactivity. This is consistent with earlier observations that pulsed electric fields with fast rising voltage pulses and narrow pulse widths from tens to hundreds of nanoseconds are particularly promising

to propel the electron temperature to notably higher levels.^{51–54} For the sine-wave excitation case, one can assume that the electric field strength inside the syringe is the same as the pulsed dc case when the applied sinusoidal voltage reaches its peak value (also 8 kV). Based on the same assumption in the pulsed dc case, the drift velocities of electrons and ions are also about 10^7 and 10^5 cm/s, respectively. During the discharge duration (about 2 μ s), the electrons and ions can be displaced by approximately 20 and 0.2 cm, respectively. This result may be an overestimate because the actual electric field should be reduced due to the adverse effects of space charges accumulated on the barrier surface. Thus, compared with the length of the SWEPs (2.4 cm), the ions can be also considered immovable. However, due to the relative long rise phase of the applied voltage (60 μ s), the electrons will obtain energy at a lower rate due to the relatively slow increase in the electric field strength compared with the pulsed dc case. That will result in a relatively low electron energy. Given that the electron density is also quite low, one can expect the formation of a fairly short plasma jet with a relatively low efficiency of the reactive species generation.

Another important point is the increased power transfer efficiency of the pulsed dc excited plasmas which feature two distinctive and consecutive discharges during the positive and negative voltage phases. Here, we stress that the discharge during the negative voltage pulse is ignited even without energy input from the external circuit. This is why the power transfer efficiency is higher in the PDCPs case as compared with the ac sine-wave-driven plasmas. The higher degree of nonequilibrium and power transfer efficiency of the pulsed dc-excited plasmas result in a substantially enhanced plasma chemistry underpinned by the higher rates of reactive species generation, which in turn is evidenced by the higher intensities of the optical emission from the helium discharge in open air. In addition, the PDCP bullets propagate faster and are longer compared to the ac sine-wave-excited plasmas.

V. CONCLUSION

We have presented the results of a comparative analysis of the most important characteristics of the two open-air helium plasma jet plumes in the same source configuration driven by the pulsed dc and ac sine-wave excitation sources in the same discharge configuration. First, the pulsed dc-excited plasma plume is about two times longer than the SWEP plume. Moreover, the discharge current of the pulsed dc-excited plasmas is about two orders of magnitude larger compared with the sine-wave-generated counterpart. This large difference in the discharge current indicates that much more electrons are produced in the PDCPs. Second, the optical emission spectrum of the pulsed dc-excited plasma plume has a markedly higher intensity than in the sine-wave excitation case. Therefore, the pulsed dc-generated discharges feature the substantially higher plasma generation efficiency than the sine-wave-excited plasmas. Third, the gas temperature of the pulsed dc-excited plasma plume is more stable and remains very close to room temperature even

when a treatment object is placed on the way of the plasma jet propagation. Meanwhile, the gas temperature of the SWEPs tends to be several tens degrees above the room temperature. This is why the pulsed dc-excited plasmas are better suited for temperature-sensitive biomedical applications than the sine-wave-generated discharges. We have also reported the results of the real-time, high-speed imaging of the dynamics of the two plasma plumes of our interest. It has been found that the plasma bullets propagate with a larger velocity in the PDCP case. The peak-value of the bullet velocity turns out to be about two times larger than in the sine-wave excitation case. Finally, the *staphylococcus aureus* bacteria inactivation process has been carried out to compare the sterilization efficiency of the two plasma plumes. It is found that for both the direct and indirect treatments, the pulsed dc-excited plasma plume is more effective in the inactivation process of the bacterial samples than the sine-wave-excited plasma plume. These results are relevant to a large number of applications in the rapidly emerging area of the plasma health care.

ACKNOWLEDGMENTS

This work was partially supported by the National Natural Science Foundation under Grant No. 10875048, the Chang Jiang Scholars Program, Ministry of Education, People's Republic of China, the Australian Research Council, and CSIRO (Australia).

- ¹G. Fridman, G. Friedman, A. Gutsol, A. Shekhter, V. Vasilets, and A. Fridman, *Plasma Processes Polym.* **5**, 503 (2008).
- ²M. Laroussi, *Plasma Processes Polym.* **2**, 391 (2005).
- ³G. Fridman, A. Brooks, M. Balasubramanian, A. Fridman, A. Gutsol, V. Vasilets, H. Ayan, and G. Friedman, *Plasma Processes Polym.* **4**, 370 (2007).
- ⁴F. Iza, G. Kim, S. Lee, J. Lee, J. Walsh, Y. Zhang, and M. Kong, *Plasma Processes Polym.* **5**, 322 (2008).
- ⁵Z. Machala, I. Jedlovsky, L. Chladekova, B. Pongrac, D. Giertl, M. Janda, L. Sikurova, and P. Polcic, *Eur. Phys. J. D* **54**, 195 (2009).
- ⁶R. Dorai and M. Kushner, *J. Phys. D* **36**, 666 (2003).
- ⁷P. Chu, *IEEE Trans. Plasma Sci.* **35**, 181 (2007).
- ⁸K. Ostrikov, *Rev. Mod. Phys.* **77**, 489 (2005); Q. J. Cheng, S. Xu, J. Long, and K. Ostrikov, *Appl. Phys. Lett.* **90**, 173112 (2007).
- ⁹Z. Machala, E. Marode, M. Morvova, and P. Lukac, *Plasma Processes Polym.* **2**, 152 (2005).
- ¹⁰C. Jiang, A. Mohamed, R. Stark, J. Yuan, and K. Schoenbach, *IEEE Trans. Plasma Sci.* **33**, 1416 (2005).
- ¹¹P. Bruggeman, J. Liu, J. Degroote, M. Kong, J. Vierendeels, and C. Leys, *J. Phys. D* **41**, 215201 (2008).
- ¹²P. Bruggeman and C. Leys, *J. Phys. D* **42**, 053001 (2009).
- ¹³R. Vidmar, *IEEE Trans. Plasma Sci.* **18**, 733 (1990).
- ¹⁴M. Laroussi and T. Akan, *Plasma Processes Polym.* **4**, 777 (2007).
- ¹⁵M. Laroussi and X. Lu, *Appl. Phys. Lett.* **87**, 113902 (2005).
- ¹⁶M. Teschke, J. Kedzierski, E. Finantu-Dinu, D. Korzec, and J. Engemann, *IEEE Trans. Plasma Sci.* **33**, 310 (2005).
- ¹⁷X. Lu, Z. Jiang, Q. Xiong, Z. Tang, X. Hu, and Y. Pan, *Appl. Phys. Lett.* **92**, 081502 (2008).
- ¹⁸D. Mariotti, *Appl. Phys. Lett.* **92**, 151505 (2008); K. Ostrikov, M. Y. Yu, and L. Stenflo, *Phys. Rev. E* **61**, 782 (2000).
- ¹⁹J. Kolb, A. Mohamed, R. Price, R. Swanson, A. Bowman, R. Chiavarini, M. Stacey, and K. Schoenbach, *Appl. Phys. Lett.* **92**, 241501 (2008).
- ²⁰Z. Kiss'ovski, M. Kolev, A. Ivanov, S. Lishev, and I. Koleva, *J. Phys. D* **42**, 182004 (2009).
- ²¹H. Lee, G. Kim, J. Kim, J. Park, J. Lee, and G. Kim, *J. Endod.* **35**, 587 (2009).
- ²²X. Lu, Z. Jiang, Q. Xiong, Z. Tang, and Y. Pan, *Appl. Phys. Lett.* **92**, 151504 (2008).

- ²³J. Walsh and M. Kong, *Appl. Phys. Lett.* **91**, 221502 (2007).
- ²⁴Z. Cao, J. Walsh, and M. Kong, *Appl. Phys. Lett.* **94**, 021501 (2009).
- ²⁵T. Kasih, S. Kuroda, and H. Kubota, *Chem. Vap. Deposition* **13**, 169 (2007).
- ²⁶Y. Hong and H. Uhm, *Appl. Phys. Lett.* **89**, 221504 (2006).
- ²⁷Q. Nie, C. Ren, D. Wang, and J. Zhang, *Appl. Phys. Lett.* **93**, 011503 (2008).
- ²⁸D. Kim, J. Rhee, B. Gweon, S. Moon, and W. Choe, *Appl. Phys. Lett.* **91**, 151502 (2007).
- ²⁹A. Shashurin, M. Shneider, A. Dogariu, R. Miles, and M. Keidar, *Appl. Phys. Lett.* **94**, 231504 (2009).
- ³⁰B. Sands, B. Ganguly, and K. Tachibana, *Appl. Phys. Lett.* **92**, 151503 (2008).
- ³¹E. Stoffels, A. Flikweert, W. Stoffels, and G. Kroesen, *Plasma Sources Sci. Technol.* **11**, 383 (2002).
- ³²E. Stoffels, Y. Sakiyama, and D. Graves, *IEEE Trans. Plasma Sci.* **36**, 1441 (2008).
- ³³X. Lu, T. Ye, Y. Cao, Z. Sun, Q. Xiong, Z. Tang, Z. Xiong, J. Hu, Z. Jiang, and Y. Pan, *J. Appl. Phys.* **104**, 053309 (2008).
- ³⁴X. Lu, Y. Cao, P. Yang, Q. Xiong, Z. Xiong, Y. Xian, and Y. Pan, *IEEE Trans. Plasma Sci.* **37**, 668 (2009).
- ³⁵J. Lim, H. Uhm, and S. Li, *Phys. Plasmas* **14**, 093504 (2007).
- ³⁶A. Shashurin, M. Keidar, S. Bronnikov, R. Jurjus, and M. Stepp, *Appl. Phys. Lett.* **93**, 181501 (2008).
- ³⁷H. Yu, S. Perni, J. Shi, D. Wang, M. Kong, and G. Shama, *J. Appl. Microbiol.* **101**, 1323 (2006).
- ³⁸Y. Hong, W. Kang, Y. Hong, W. Yi, and H. Uhm, *Phys. Plasmas* **16**, 123502 (2009).
- ³⁹T. Sato, T. Miyahara, A. Doi, S. Ochiai, T. Urayama, and T. Nakatani, *Appl. Phys. Lett.* **89**, 073902 (2006).
- ⁴⁰M. Laroussi, C. Tendero, X. Lu, S. Alla, and W. Hynes, *Plasma Processes Polym.* **3**, 470 (2006).
- ⁴¹M. Laroussi, *IEEE Trans. Plasma Sci.* **37**, 714 (2009).
- ⁴²K. Weltmann, E. Kindel, R. Brandenburg, C. Meyer, R. Bussiahn, C. Wilke, and T. Woedtke, *Contrib. Plasma Phys.* **49**, 631 (2009).
- ⁴³G. Fridman, A. Shereshevsky, M. Jost, A. Brooks, A. Fridman, A. Gutsol, V. Vasilets, and G. Friedman, *Plasma Chem. Plasma Process.* **27**, 163 (2007).
- ⁴⁴G. Kim, G. Kim, S. Park, S. Jeon, H. Seo, F. Iza, and J. Lee, *J. Phys. D* **42**, 032005 (2009).
- ⁴⁵H. Lee, C. Shon, Y. Kim, S. Kim, G. Kim, and M. Kong, *New J. Phys.* **11**, 115026 (2009).
- ⁴⁶S. Deng, R. Ruan, C. Mok, G. Huang, X. Lin, and P. Chen, *J. Food Sci.* **72**, M62 (2007).
- ⁴⁷S. Perni, W. Liu, G. Shama, and M. Kong, *J. Food Prot.* **71**, 302 (2008).
- ⁴⁸X. Lu and M. Laroussi, *J. Appl. Phys.* **100**, 063302 (2006).
- ⁴⁹R. Ye and W. Zheng, *Appl. Phys. Lett.* **93**, 071502 (2008).
- ⁵⁰Y. Raizer, *Gas Discharge Physics* (Springer-Verlag, New York, 1991).
- ⁵¹S. Liu and M. Neiger, *J. Phys. D* **34**, 1632 (2001).
- ⁵²M. Laroussi, X. Lu, V. Kolobov, and R. Arslanbekov, *J. Appl. Phys.* **96**, 3028 (2004).
- ⁵³R. Mildren, R. Carman, and I. Falconer, *J. Phys. D* **34**, 3378 (2001).
- ⁵⁴R. Carman and R. Mildren, *J. Phys. D* **36**, 19 (2003).